Design of FUZZY-3DOF-PID controller for an Ocean Thermal hybrid Automatic Generation Control system

Susmit Chakraborty[a], Arindam Mondal[b*], Soumen Biswas[b] and Provas Kumar Roy[c]

[a] Electrical& Electronics Engineering Department, Pailan College of Management & Technology, Kolkata, India

[b] Electrical Engineering Department, Dr. B C Roy Engineering Collee, Durgapur, India

[c] Electrical Engineering Department, Kalyani Government Engineering College, Kalyani, India

Highlights

- A 3-area hybrid power system network containing Ocean thermal power source as a renewable energy source is proposed.
- The Fuzzy controller cascaded with 3DOF-PID (FUZZY-3DOF-FOPID) is proposed as a new control scheme for LFC studies.
- Firebug Swarm Optimization meta-heuristic algorithm is applied to tune the proposed controller.
- Better results of frequency errors and tie-bar power errors are obtained in terms of over-shoot, under-shoot and settling time.
- The proposed controller is found to be robust with the variation of Random Load Perturbation (RLP) and with the variation of system parameters.

Abstract

Balancing generation and demand are the most essential requirement for a power system (PS). Both the changes in loads and the sources included into the PS affect the frequency of generation. The PS that is integrated with various non-renewable and renewable energy (RE) sources must be reliable and under control with minimal load fluctuations. The automatic generation controller (AGC), which is essential for achieving frequency balance in the PS. A mismatch of frequency between the supply and demand may lead to development of system errors. In this paper, an intelligent, robust Fuzzy logic-based controller is proposed for AGC in PS incorporating different RE sources like solar, wind, and ocean-thermal. Controller parameters are optimally tuned using nature-inspired, meta-heuristic algorithm known as Firebug Swarm Optimization (FSO). A 2-area-test system containing thermal, hydro and gas power-plant is considered as the test bench for the proposed controller. Later on, a fuzzy 3DOF-PID

Corresponding Author: arininstru@gmail.com *(Arindam Mondal), +919733722500,*
E-mail: susmit.eee@gmail.com *(Susmit Chakraborty), +917980492839,* soumeniitkgp10@gmail.com *(Soumen Biswas), +916290191294,* roy_provas@gmail.com *(Provas Kr. Roy), +919474521395*

controller is designed for controlling 3-area PS containing RE sources like solar, wind, and ocean-thermal along with the hydro, thermal, and nuclear units. The designed controller is robust to load variation and the comparison of the various indices demonstrates the superiority of the proposed controller over other controllers available in literature.

Key words: Automatic generation control (AGC). Firebug Swarm Optimization (FSO). FOPID Controller. Fuzzy. Non-renewable energy sources. 3-degree freedom of PID (3DOF-PID).

Nomenclature and Abbreviations:

α_{ij}= control area size ratio.
β_i : Characteristics of frequency response
ΔF_i : Frequency variation in the control area
ΔP_{tieij} : Tie-line power flow deviation
ACE: Area control error
ACE-D: Area control error-Derivative
AE-FC: Aqua-electrolyser-fuel cell
AGC: Automatic Generation Control
ASO: Atomic search algorithm
BFA: Bacteria foraging algorithm
DW: Derivative control set point
EV: Electric Vehicle
FES: Fly-wheel energy storage
FIS: Fuzzy interface system
FLC: Fuzzy logic controller
FSO: Firebug swarm optimization
GOA: Grasshopper optimization algorithm
G_{ff} : forward gain of disturbances
IAE: Integral of absolute error
ICA: imperialist competitive algorithm
ISE: Integral of squared error
ITAE: Integral of time multiplied absolute error
ITSE: Integral of time multiplied squared error
K_d : Derivative Coefficient
K_p : Proportion Constant
K_i : Integral Constant
MSHTS: Multi-source non-reheat thermal system
OS: Over shoot
PW: Proportional control set point
RE: Renewable Energy
SCA: Sine-Cosine algorithm
ST: Setting time
SLP: Step load perturbation
UC: Ultra capacitor

1. Introduction

Gradual abatement of energy resources and increment of load demands pose a challenge to the power generation and controlling sector [1]. Energy demand induces very high dangers to the Power System (PS) stability. It causes the sluggish speed of the turbine as well as a decline in the frequency of the output voltage of the alternator. A common frequency in all generation units of interconnected large-scale PS is desired. Generating units should be connected synchronously with a fixed actuation frequency. Thus, it is desirable to sustain zero frequency error and error-less tie-bar power in the inter-connected PS network. To satisfy this need, automatic generation control (AGC) strategy of continuous manipulation of the valve of the steam or hydro turbine should be implemented in the system [2]. The PS network is becoming more and more complex as RE sources like solar, wind, geothermal, and ocean thermal are added to the interconnected PS network. Nowadays, fossil fuel resources are depleted with the enhanced use of RE sources in PS industry. RE sources are much environment-friendly and also ample in nature. Furthermore, the energy conversion efficiency of the RE sources is swelling with the shrinking of the cost day-by-day [3]. Solar and wind are the most extensively used sources among all RE sources. Hence, solar and wind energy have become prominent areas of curiosity for researchers. A dish-Stirling hybrid system containing solar and thermal units in AGC has been studied by Rahman et al. in [3]. Two area PS having reheat-thermal, solar, wind, aqua-electrolyser-fuel cell (AE-FC) units have been studied by Kler et al. in [4]. A hybrid Power system network consisting of different types of RE Sources like Wind turbine generator, solar-thermal generator, solar cell, diesel-engine generator, AE, fuel cells, battery energy storage (BES) system, Fly-wheel energy storage (FES) system and ultra-capacitor (UC) are presented in detail in [5]. AGC incorporating inter-connected power system units like solar-reheat thermal, hydro-thermal, multi-source non-reheat thermal system (MSHTS) with AE-FC units are analyzed in [6]. The effects of solar-thermal generators and geothermal units are analyzed in two and three area-deregulated PS [7, 8]. A delay-based PI controller in deregulated PS network with renewable energy and storage device is demonstrated in [9]. Electric vehicle (EV) along with hybrid sources like thermal, wind, hydro, and solar in the Guangdong power grid is discussed in [10]. AGC in power sectors ensures the system's reliability and power quality and provides brisk and stress-less control over interconnected multi-area PS networks. Incorporation of RE system demands a robust and highly efficient strategy to control and maintain stability in presence of the variational nature of RE system. To meet the objective of AGC, different controlling techniques, as well as tuning methods, are available in the literature. Since PSs are strongly affected by the weather conditions like temperature, Barometric pressure, humidity etc. the conventional controllers might not work properly. These are responsible for the de-synchronization, and communication delay in the output power with the interconnected grid. To overcome this problem and to meet higher efficiency levels in frequency and tie-bar power in PS networks, intelligent controlling action like a Fuzzy-logic controller (FLC) is considered instead of a conventional type controller [6]. FLC is an Intelligent multi-valued powerful controlling technique that can sense small deviations in frequency and tie-bar power and handle system operation efficiently [11]. A crucial step is selecting FLC parameters including scaling factors (SFs), membership functions (MFs), and governing rules. These parameters are chosen as per the operator's experimental statistics. An adverse effect of system output might be seen by selecting inappropriate factors. Hence, various optimization techniques are intelligently applied in different PS network for setting optimum values of the parameters of Fuzzy-logic controller. Recently many optimization methods are implemented for tuning SFs of Fuzzy based controllers in AGC like BFOA [12], hPSO-LFA [13], hHS-COA [14], hIFAPS [15], hDE-PSO [16]. Popularity of Fractional-Order Controllers (FOC) is rapidly increasing day by day due to its skillful operation to control errors in PS networks. It is already verified the superiority of FOC over Integer order (IO) controllers [11, 17-21]. Recently FOC are used in AGC problems and it gives satisfactory results for the last few years. A FOFPID controller is used in AGC using ICA [18], BFOA [19], and QOHSA [20] and shows improved results compared to the controlling actions of conventional type controllers. Further, some cascaded controllers like FOPI-FOPID [7], FOPIFOPD [8], PIDN-FOPD [22], and FFOPI-FOPD [23] have appeared in recent literature. Different optimization methods are required to tune the controllers for AGC. The available optimization methods include carrier-inspired-algorithm (CIA) optimized I/PI/ID controller [2], CASO optimized PI controller [9], BFA optimized PI controller [24], GSA optimized PI controller [25], GOA optimized 3DOF-PID controller [26], SCA optimized PID with Fuzzy logic controller (FUZZY-PID) [27], Fuzzy enabled ICA optimized PID controller [11], Fuzzy Adaptive Fixed-time Sliding Mode Control [28], Fuzzy gain scheduling PID control [29], Fractional-order fuzzy PID controller design on buck converter with antlion optimization algorithm [30]. Firebug Swarm Optimization (FSO) is a new algorithm that can be utilized to adjust the various controller parameters in the AGC system. It is a global optimization algorithm with biological inspiration that uses no derivatives. It is inspired by reproductive swarming behavior of Firebugs [31,32,33,34]. It is advantageous to quickly tackle large-scale optimization problems with higher dimensions (above 100). It can be successfully used to solve issues in the real world, including the design of mechanical structures, the design of filters, controllers, and the optimization of power system networks [35].

The following section discusses the significant contribution of this work. This paper deals with a new renewable energy source like Ocean Thermal energy source. The Fuzzy logic-based 3DOF-PID controller is designed in this work for the satisfactory operation of an ocean-thermal-based hybrid PS network. 3 degrees of freedom for fractional order PID controllers are tuned using a biologically inspired meta-heuristic algorithm called Firebug Swarm Optimization (FSO). The tested controller is first employed on a two-area test system before being applied to a three-area hybrid PS network. Comparing the outcomes of the suggested approach with those of other controllers found in the literature demonstrates its strength. The robustness study proves the superior performance of the controller in handling any kind of disturbance. The taxonomy regarding the load frequency control using different controllers tuned with various types of optimization algorithm is summarized to have a clear picture about the trends of research in the focused area in Table1.

2. Motivation of the Work

In recent research, the renewable sources are the main focus which are considered as the sources of energy in power system network. But the use of ocean thermal energy as an energy source in the hybrid power system remains in its preliminary stage. The generation of nonlinearities due to renewable sources is the major problem to use of it. There should be a controller that can reduce the nonlinearities of the system. Fuzzy control has been one of the most vibrant and productive fields for study in the use of fuzzy set theories during the past couple of decades. The fundamental tenet of this strategy was to develop the controller while taking into account the "learning" of a human process of operations. A control algorithm is built from a collection of linguistic rules that characterize the operator's controlling approach, with the words described as fuzzy sets. Fractional order controllers are capturing the domain of LFC day by day. The authors have been motivated to work on load frequency controller design by the gathering the concepts of fuzzy logic and fractional order calculus, particularly in the interconnected network with Ocean Thermal energy source as one of the important renewable energy sources.

3. Power system model for LFC

A 2-area test system and a 3-area hybrid system are considered in this work. In this system, 2 area test system contains 3 units like thermal, hydro and gas for each area, which is given in Fig. 1. The ratings of each unit for each area in the test system are considered as, thermal: 2000 MW, hydro: 1000 MW, gas: 500 MW. For a 3-area hybrid system, the ratings are as, solar: 1000 MW, thermal: 2000 MW, ocean-thermal: 1500 MW, nuclear: 1500 MW, wind: 1000 MW, hydro: 2000 MW. Nominal nomenclature and parameters of both systems are elucidated in the Appendix.

4. Controller design

This study implements a cascade combination of fuzzy based PID and fuzzy-based 3DOF-PID controllers for LFC of a 3-area power system network. Area Control Error (ACE) and its derivatives (ACE-D) are used as-input variables to the Fuzzy logic controller (FLC).

4.1 Fuzzy Logic Controller

Fuzzy is a powerful intelligent multivalued logical operation that deals with imprecise granular information from a set of data collection. For this work, the linguistic information is taken from the previously designed fuzzy control by Gupta et al. [36]. There are four components such as fuzzifier, knowledge base, inference system and de-fuzzifier in Fuzzy logic controller. Fig. 2 shows a generalized block diagram of a fuzzy inference system (FIS). Operation of fuzzy starts with fuzzifier operation where input signals are converted into fuzzy values. These fuzzy values are the input to the inference system which is used as the reasoning and value setting operation of the controller. It takes appropriate output making decisions using rule-base. Rule-base is basically a set of information present in the membership function of the Fuzzy system, and known as Knowledge base. After taking decisions, the outputs in terms of fuzzy values are converted into real life values or crisp values using de-fuzzifying operation. Fuzzy set variables are denoted using the combinations of letters and called as linguistic variable. The linguistic variables in this work are represented by the letters NL, NM, NS, ZR, PS, PM & PL, and they stand for negative large, medium, small, zero and positive small, medium, and large, respectively. To obtain the true control output of the FLC, the Mamdani fuzzy inference system and the center of gravity approach of defuzzification are applied.

FLC acts as the scaling factors (SF) [37] for the input signals of the controller. This will increase the efficiency of controller tuning rather than the optimization of the shape of membership functions (MF). In this work, the shape of the MF and rule base for controller tuning are considered constant for Fuzzy-PID as well as Fuzzy-3DOF-PID controller design. The fuzzy rule-base utilized for the design of Fuzzy-PID and Fuzzy-3DOF-PID controller is illustrated in Table 2 [11]. Fig.3 displays the fixed-shaped MFs for inputs and FLC output and Fig.4 defines the surface generation of all probable combinations of input set.

For the successful implementation of controller, optimized tuning of the controller parameters is primary concern. There is no straight forward rule for the optimization of MFs of FLC. In this work, four different time integral performance indices (Q_s) are incorporated for the optimization purpose. These are as follows.

$$Integral\ of\ absolute\ error\ (IAE) = \int_0^{\infty} \{ |\Delta F_1| + |\Delta F_2| + |\Delta P_{tie12}| \} dt$$

(1)

$$Integral\ of\ time\ multiplied\ absolute\ error\ (ITAE) = \int_0^{\infty} t \{ |\Delta F_1| + |\Delta F_2| + |\Delta P_{tie12}| \} dt \tag{2}$$

$$Integral\ of\ square\ error\ (ISE) = \int_0^{\infty} \{ \Delta F_1^2 + \Delta F_2^2 + \Delta P_{tie12}^2 \} dt \tag{3}$$

$$Integral\ of\ time\ multiplied\ square\ error\ (ITSE) = \int_0^{\infty} t \{ \Delta F_1^2 + \Delta F_2^2 + \Delta P_{tie12}^2 \} dt \tag{4}$$

The performance indices (Q_s)are scripted here for a 2-area test system and same set of notations can be scripted for 3 area hybrid system. In this paper, the Fuzzy-PID and Fuzzy-3DOF-PID controller parameters are optimized using the ISE, ITSE, IAE and ITAE as Q_s are subjected to the six different variables. A constrained optimization problem is devised according to following constraints: minimize $Q_s$subject to

$$K_P^{min} \leq K_P \leq K_P^{max}, K_I^{min} \leq K_I \leq K_I^{max}, K_D^{min} \leq K_D \leq K_D^{max}, PW^{min} \leq PW \leq PW^{max},$$
$$DW^{min} \leq DW \leq DW^{max}, N^{min} \leq N \leq N^{max}$$

The smallest and highest value of the controller parameters are represented by the min and max symbols. Firebug Swarm Optimization (FSO) algorithm is used in this work to tune the above-mentioned parameters. The Convergence analysis of the proposed algorithm using ISE criterion for three different control logics is illustrated in Fig. 5.

4.2 Fuzzy-PID controller

A simple PID controller is cascaded with the FLC and act as a single controller unit as described by Equation 5. The parameters K_p, K_i, K_d for PID controllers are optimally tuned using FSO algorithm. Considering the output of the FLC (Y), the output of the Fuzzy-PID controller is demonstrated by Equation 6.

$$PID = K_p + sK_d + \frac{K_i}{s}$$

(5)

$$C_{out} = Y*(K_p + sK_d + \frac{K_i}{s})$$

(6)

4.3 Fuzzy-3DOF-PID Controller

Fig. 6 depicts the structural layout of 3DOF-PID controller. It is a 3-degrees-of-freedom associated PID controller where $R(s)$ represents reference input to the controller, $Y(s)$ is the tie-bar power feedback signal and $D(s)$ is considered an external noise signal. Main objective of this controller is to reject high disturbances, considering the dynamic response as well as close loop stability [36]. Two parameters represented as PW and DW are the set-points of proportional and derivative controllers respectively. `N' is the coefficient of the derivative low pass filter. G_{ff} is a forward gain of disturbances ($D(s)$) applied externally. ΔP_C = output from the 3DOF-PID controller and is expressed by Equation 7.

$$\frac{\Delta P_C(s)}{R(s)} = \frac{s^2\left(K_d N*DW + K_p*PW\right) + s\left(N*PW + K_i\right) + K_i N}{s(s+N)}$$

(7)

Fig. 7 provides an illustration of the Fuzzy-3DOF-PID controller structure. For Fuzzy-3DOF-PID, output of Fuzzy block is considered as reference input $R(s)$ to the 3DOF-PID controller block. The parameters, K_p,K_i, K_d and N of 3DOF-PID controllers are tuned using FSO technique. The ACE for systems with 2 and 3 areas are expressed below.

For 2-area test system,

$$\left.\begin{aligned} ACE1 &= \beta_1 \Delta F_1 + \Delta P_{tie12} \\ ACE2 &= \beta_2 \Delta F_2 + \alpha_{12} \Delta P_{tie12} \end{aligned}\right\}$$

(8)

For 3-area system,

$$\left.\begin{aligned} ACE1 &= \beta_1 \Delta F_1 + \Delta P_{tie12} + \Delta P_{tie13} \\ ACE2 &= \beta_2 \Delta F_2 + \Delta\alpha_{12}\Delta P_{tie12} + \Delta P_{tie23} \\ ACE3 &= \beta_3 \Delta F_3 + \Delta\alpha_{13}\Delta P_{tie13} + \Delta P_{tie23} \end{aligned}\right\}$$

(9)

Where β_i= characteristics of frequency response, ΔF_i= frequency variation in the control area, ΔP_{tieij} = tie-line power flow deviation, α_{ij}= control area size ratio.

5. Firebug Swarm Optimization (FSO) Algorithm

In this study, the controller parameters are optimized using the Firebug Swarm Optimization (FSO) algorithm [35]. FSO is a new method of optimization influenced by biology that was created by analyzing the reproductive swarming activity of firebugs (Pyrrhocorisapterus). It is a derivative free global optimization algorithm. A swarm of Firebugs' individual bugs are attempting to find the most suitable mates, and this is seen as a natural search for the best answer in the overall search space. There are two distinct types of firebug behavior (Pyrrhocorisapterus). They either wander and explore alone or exhibit gregariously aggressive behavior when forming groups. The aggregations aid firebugs in reducing predation and locating the most compatible mates for reproduction. Firebugs perform these aggregations generally in summer season. The behavior of Firebugs can be described in five major steps. The steps are described below.

Step1: Formation of female firebug colonies

The objective of this optimization procedure is to reduce the cost function for finding compatible partners. Fittest mate is always present with low-cost value. F female bugs and M male bugs are randomly scattered around the search space to begin the optimization. Each bug is paired with a cost function and a position vector (modelled as a column vector).

Step2: Mate selection

Random selection of a male bug with the fittest female bug is done and their location is initialized. The fittest selection is searched in a colony of male bugs and updated each step for a better result. The updated location of the fittest male bug is obtained using elementwise Hadamard Matrix Multiplication

Operation (HMMO). This will ensure the parallel and faster operation of CPU and GPU by the Single Instruction Multiple Data (SIMD) feature. Thus, execution time is drastically reduced for a set of operations. The position vectors of individual bugs are passed as a single matrix when the CEC 2017 test suite is activated, thereby making the cost functions evaluation a highly vectorized one. To speed up processing, several high-level language computing platforms, such as MATLAB and Python, use matrices rather than scalars [39-41].

Step3: Movement of female bugs chemotactically

According to the female bugs' chemotactic behavior, the location of the female bug is updated. The female bugs in a colony of male bugs are drawn to the leaders more than the weaker male bugs. To prevent wasteful scalar operations, the FSO approach uses matrix operations. In a matrix, the locations of the female bugs in a specific colony are recorded and updated simultaneously. Let $p(p).F$ be the $d\ x\ F$ matrix whose columns represent position of female bugs. The Hadamard multiplication procedure is performed with the following equations to update all female bugs in a fixed colony simultaneously.

$$P_x \leftarrow repmat(p(p).x,\ 1, F)$$

$$P_Y \leftarrow repmat(p(a).x,\ 1, F)$$

where a = random integer ranging between 1 and F. The function $repmat\ (A, p, q)$ gives back a matrix which contains p copies of A in row dimension and q copies in column dimension. Thus, if A is a $m\ x\ n$ matrix, then $repmat\ (A, p, q)$ returns one $pm\ x\ qn$ matrix.

$$p(p).F \leftarrow p(p).F + C1 \odot \left(P_X - p(p).F\right) + C2 \odot \left(P_Y - p(p).F\right) \quad (10)$$

For the better performance of FSO, the values of C_1 are taken significantly larger than the values of C_2.

Step4: Attraction of male-Firebugs to fittest female bugs

Female bugs which are fitted well also attract male bugs, not in its colony. This male movement keeps the entire population constrained to one area and prevents a swarm of it. In a specific male bug colony, there is no competition between the fittest female bugs. This activity prevents to premature convergence of the algorithm by preventing attraction of male bugs towards a particular female bug. The following is the update rule that directs male bugs toward the fittest female bugs:

$$p(p).X \leftarrow p(p).X + C3\, \Theta\, (\, k - p(p).X) \quad (11)$$

Step5: Swarm cohesion

Swarm cohesion is a phenomenon where entire swarm move together in a single direction in a stochastic manner. The proposed model of the herd cohesion can be represented by Equation 12. According to Equation 12, each male bug is following the movement of a random male bug which is again attracted by fittest female bug. In the FSO method, the male bug moves and copies the motion of another male bug to provide the optimum solutions, preventing an early convergence to a local minimum.

$$p(p).X \leftarrow p(p).X + C4\, \Theta(\, k - p(b).X) \quad (12)$$

The FSO algorithm is a method of optimization inspired by nature in which firebugs try to find the optimal reproduction partner through swarming behavior. The search of the ideal partner can be compared to the pursuit of the ideal response in the search space. The simplest equation for update of activity for the reproductive swarming of firebug is as follows:

$$X = X_1 + \alpha\left(X_2 - X_1\right) = (1 - \alpha)X_1 + \alpha X_2 \quad (13)$$

Fig. 8 represents the movement of the point X (position of the bug) in the range from X_1 to X_2 with the variation of α from $0\ to\ 1$. For $\alpha > 1$, the point X, moves right towards X_2 on the line joining X_1 and X_2. For $\alpha < 0$, the point X, moves left towards X_1 along the same line. For different values of α, the point X traces different positions along the line joining X_1 and X_2.Using Fig. 8 and Equation 13, the vector X can be calculated by applying the triangle law of vector addition. Therefore, male bug moves (with position $(p(p).x)$ towards the fittest female bug (with position k) with a predefined equation as given by,

$$p(p).X \leftarrow p(p).X + \alpha(\, k - p(p).X) \quad (14)$$

To improve the process of independent exploration in various dimensions Equation 14 is updated and replaced by Equation 15.

$$p(p).X \leftarrow p(p).X + C4\,\Theta\,(\,k - p(b).X)$$

(15)

The strong and weak movements of the female bug towards fittest male and random males respectively can be expressed by Equation 16.

$$p(p).F \leftarrow p(p).F + C1\,\Theta\left(P_X - p(p).F\right) + C2\,\Theta\left(P_Y - p(p).F\right)$$

(16)

In the right-hand side of Equation 16, the word including C_1 denotes the female bug's movement toward the dominant male bug, whereas the term containing C_2 denotes the female bug's movement toward an undetermined male bug. The matrices C_1 and C_2 are used to denote the degree of attraction towards dominant male bug and random male-bug respectively by female-bugs. Fig. 9 illustrates the flowchart for FSO algorithm.

6. Simulation Results

The systems are designed and tested using MATLAB/SIMULINK version 2020A with Intel (R) Core (TM) i7-1065G7 CPU @ 2.80 GHz processor with 16 GB RAM memory were used to run the simulations. The settings of the MATLAB simulation are considered as variable step ODE45 type solver. The simulation time for each iteration is taken as 70 Second. Fuzzy PID and Fuzzy 3DOF-PID controller settings are tuned using the FSO technique.

6.1 2-area thermal-hydro-gas power system

Fig.1 illustrates the two-area integrated power system. This system, which employs the FSO algorithm, is regarded as a test system. This system uses four different types of controllers for load frequency control, including PID, Fuzzy-PID, FOPID, and Fuzzy-3DOF-PID (proposed). The parameters of all the controllers are tuned using FSO. The optimized parameters of four different controllers are enumerated in Table 3. The responses of the frequency error (ΔF_s) and tie-bar power error (ΔP_{tie12}) of the system for different controllers are consolidated in Fig.10. From this figure, it is clearly seen that the Fuzzy-3DOF-

PID controller outperforms the other controllers regarding less oscillation, peak undershoot, peak overshoot and settling time. The time domain parameters for checking the system performance are tabulated in Table 3. The frequency error (ΔF_1) of the 1st area is illustrated in Fig. 10(a) whereas, Fig. 10(b) shows the frequency error (ΔF_2) of the 2nd area of the system. Fig. 10(c) represents tie-bar power error *(*ΔP_{tie12}) between these two areas and the Fuzzy-3DOF-PID controller has been discovered to provide better control of the system with the least amount of overshoot *(*OS*)*, undershoot (US), and settling time *(*ST*)*.

The Fuzzy-3DOF-PID controller tuned by the FSO algorithm is superior, as evidenced by an examination of the parameters displayed in Table 4, where the frequency deviation in area-1 is indicated by $OS = 0.000961\,Hz$, $US = -0.008401\,Hz$, and $ST = 20.56\,second$. Similarly for area- 2, the values of parameters are $OS = 0.000753\,Hz$, $US = -0.006432\,Hz$ and $ST = 20.11\,second$. The tie-bar error is also less using the proposed controller and the numerical values of $OS/US/ST$ are $0.000714\,Hz$, $-0.00513\,Hz$ and $20.06\,second$ respectively. Therefore, it is obvious that the proposed controller outperforms the other controllers. The statistics can be summarized as: The proposed controller is better by 89.90 % than PID, 83.8 % than FOPID, 86.31 % than FUZZY-PID controller considering OS of ΔF_1, better by 59.81 % than PID, 59.9 % than FOPID, 55.99 % than FUZZY-PID controller considering US of ΔF_1, better by 81.85 % than PID, 57.06 % than FOPID, 67.27 % than FUZZY-PID controller considering OS of ΔF_2, better by 61.49 % than PID, 61.47 % than FOPID, 58.62 % than FUZZY-PID controller considering US of ΔF_2. Hence, the proposed controller proves its efficacy in comparison to other controller performances.

6.2 3-Area hybrid system incorporating Ocean Thermal Energy source

A three-area hybrid system incorporating Ocean Thermal Energy source along with solar, wind, thermal, hydro and nuclear energy is demonstrated in Fig. 11. Four different controllers are used for the load frequency control of the given system. Three frequency errors (ΔF_s) and two tie-bar power errors (ΔP_{tieij}) are observed. The responses employing the Fuzzy-3DOF-PID controller have been shown to demonstrate the optimal controlling action for the 3-area hybrid system. Four different algorithms such as GOA [42], ASO [43], ICA [44] and FSO [32] are used to tune the controller parameters of Fuzzy-

3DOF-PID to prove the efficacy of the FSO algorithm over others. The data and the nomenclatures of the power system are prescribed in the Appendix. The results of the power system network under 10% step load perturbation (SLP) applied at the initial condition are listed in Table 5 in terms of error in frequency of three separate areas and the power error in tie-bar between the first-second and first-third area.

Figs. 12(a), 12(b), 12(c), 12(e) &12(f) are representing the frequency and tie-bar errors in 3-area hybrid system controlled using four different controllers. Frequency error in ocean thermal unit is demonstrated in Fig. 12(d). Table 6 shows FSO optimized controller parameters for all four controllers. Fuzzy-3DOF-PID controller proves its efficacy compared to other controllers and this could be seen from the transient parameter readings.

For 3-area system also, the proposed controller outperforms the other controllers by 89.80 % than PID, 84.02 % than FOPID, 85.97 % than FUZZY-PID controller considering OS of ΔF_1, 59.85 % than PID, 59.85 % than FOPID, 56.30 % than FUZZY-PID controller considering US of ΔF_1, 81 % than PID, 57.77 % than FOPID, 63.80 % than FUZZY-PID controller considering OS of ΔF_2, 62.11 % than PID, 61.43 % than FOPID, 57.90 % than FUZZY-PID controller for US considering ΔF_2. Hence, FUZZY-3DOF-PID controller proves its efficacy over other controllers.

Fuzzy-3DOF-PID controller is controlling the system with $OS = 0.0009518\,Hz$, $US = -0.008390\,Hz$ and $ST = 20.56\,second$ for ΔF_1 and $OS = 0.0007523\,Hz$, $US = -0.006437\,Hz$ & $ST = 20.12\,second$ for ΔF_2. Grasshopper optimization algorithm (GOA) [42], Atomic search optimization algorithm (ASO) [43], Imperialist competitive algorithm (ICA) [44] are also used to tune the FUZZY-3DOF-PID controller for 3-area hybrid system as discussed. In the next section, the findings of the frequency errors and tie-bar power deviations are contrasted with those obtained using an FSO-tuned Fuzzy-3DOF-PID controller on the same system.

The parameters such as K_p, K_i , K_d, PW, DW, N as obtained using the different optimization techniques such as GOA, ASO, ICA and FSO are depicted in Table 7. In this study, four distinct optimization strategies are used to tune the FUZZY-3DOF-PID controller. From the figures as shown in Fig. 13(a), 13(b), 13(c), 13(d) & 13(e) the frequency errors and tie-bar power errors can be observed, and it is noted that Fuzzy-3DOF-PID gives better response when tuned with FSO algorithm. GOA tuned Fuzzy-3DOF-PID gives $0.003772\ Hz, 0.002712\ Hz$ and $0.008456\ Hz$ frequency deviation in OS for 1st, 2nd and 3rd area of the hybrid system configuration respectively and the details are enumerated in Table 8. ICA tuned controller responses are better as compared to responses obtained using GOA tuning with OS of $0.0007962\ Hz, 0.0006668\ Hz, 0.004225\ Hz$ for ΔF_1, ΔF_2 and ΔF_3 respectively. Frequency errors for first two areas are not settled at zero value which is desired when tuned using GOA and ICA but the same error in the 3rd area is settled at zero value using these two algorithms. On other hand, ASO and FSO tuned controllers are providing zero frequency errors for all the three areas. Figs. 13(d) and 13(e) are demonstrating the tie bar power errors between 1st & 2nd area and 1st & 3rd area respectively. Inspection of Table 8 reveals that FSO tuned controller provides best results in connection with settling time consideration ($\Delta F_1 = 20.56\ s$, $\Delta F_2 = 20.12\ s$, $\Delta F_3 = 14.51\ s, \Delta P_{tie12} = 20.83\ s$, $\Delta P_{tie13} = 20.46\ s$).

From Table 8, some interesting comparison has been observed for the proposed controller (Fuzzy-3DOF-PID). Four different optimizations have been used to tune the parameters and the tuned controller gives better OS of ΔF_1 for ASO: Fuzzy-3DOF-PID controller by 94.03 % than GOA, 71.73 % than ICA and 76.36 % than FSO. ICA: Fuzzy-3DOF-PID gives better result in terms of US for ΔF_1 by 0.4 % than GOA, 2.4 % than ASO and 0.1 % than FSO. In case of ST for ΔF_1, FSO outperforms all controllers where GOA and ICA can`t settle fully and 9 % better result obtained than ASO.

A detailed examination of contents of Table 9 reveals that the suggested FSO-tuned FUZZY 3DOF-PID controller is superior in terms of Q_s such as ISE (0.0000468), ITSE (0.0000227), IAE (0.0062), ITAE (0.0104). The smallest values of Q_s using Fuzzy-3DOF-PID controller are represented using bold font in Table 8. FSO tuned PID controller provides worst results among all controllers considering the value of objective functions using ISE (0.0766), ITSE (0.0812), IAE (0.1823), ITAE (0.2751). FSO tuned FOPID results slightly better as compares with FSO tuned PID and the values of Q_s are like ISE (0.00992), ITSE

(0.00806), IAE (0.0472), ITAE (0.0227). With the introduction of Fuzzy logic, Q_s results have been improved as can be seen in Table 8.

7 Robustness Analysis

7.1 Robustness analysis with random load perturbation

To test the resilience of proposed Fuzzy-3DOF-PID controller, a random load type (RLP) disturbance is applied to area 2 of the hybrid power system (Fig. 11), which houses the related Ocean Thermal power system as a power producing plant. The disturbance is considered with a magnitude of ± 0.02 puMw. A comparative analysis of robust behavior among the different controllers are represented in Fig. 14. The perturbation is denoted by red line in the shown Fig.14. Closure observation of the results obtained after controlling by different controlling units under ± 0.02 puMw RLP load reveals that the proposed controller (Fuzzy-3DOF-PID) is having the best ability to retain stability among all other controllers considered under this study.

7.2 Robustness analysis with variation of system parameters

Robustness is the capacity of a system to continue operating correctly and effectively when a variety of variables are actually modified up to a particular tolerated range. The fractional controllers are inherently robust to the changes in the system parameters. In this work, the parameters of the area-2 which is composing of Ocean thermal & nuclear energy sources, are varied by $\pm 20\%$ with respect to their optimum values and the Table 10 is used to depict the changes of these parameters. It is been seen from the Fig.15 that with the variation of system parameters by $\pm 20\%$, the proposed controller provides almost same results as obtained with the optimum parameters of the system. This justifies the iso-damping behavior of the fractional order controller.

8. Conclusion

- In this script, it is attempted to use of fuzzy control strategy for controlling hybrid 3 area interconnected power system network.

- This paper deals with an interconnected power system incorporating a newly enlisted renewable energy source called as Ocean Thermal energy source.
- For the purpose of effectively resolving LFC in a linked power system network, a novel fuzzy-3DOF-PID controller is presented.
- Four different criterion such as IAE, ISE, ITSE and ITAE are considered as the error minimization functions for tuning the parameters of the proposed controller.
- FSO algorithm is used to tune the controller parameters. The proposed controller is revealed to be superior to the other controllers available in the literature in terms of dynamic response parameters like OS, US and ST. The controller has shown its supremacy in terms of minimum values of the fitness functions.
- FSO algorithm is compared with other algorithms for tuning the proposed controller and finds its superiority as can be illustrated through the Fig. 13 and Table 8.
- The designed controller is tested for its robustness, and it has proved its efficacy in this analysis as seen in Fig. 14 and Fig.15. Hence, the control strategy formulated using the optimization method and controller structure presented in this work can be a viable alternative to the existing method in LFC studies of interconnected power system network incorporating renewable energy sources

9. Appendices

Appendix A. For Test Two area system:

B_1, B_2 = 0.425p.u MW /Hz; R_1, R_2 = 2.4Hz/pu; T_{G1} = 0.08s; T_{T1} = 0.3s; T_{r1} = 10s; K_{r1} = 0.3s; $K_{P\,1}$ = 120Hz/puMW; K_{WT1} = 1.25; T_{TP1},W_{T1} = 0.65; T_{TP} 2,W_{T2} = 0.3; K_{P2} = 120Hz /pu MW; T_{P1} = T_{P2} = 20s; P_{tie12} = 200 MW; $a_{12} = -1$, RLP = ±0.02p.u(Mw) a = 900; b = −18; d = 50; d = 50.

Appendix B. For Hybrid Three area system:

B_1, B_2, B_3= 0.425p.u MW /Hz; R_1, R_2, R_3= 2.4Hz/pu; $K_{G1} = K_{G2} = K_{G3} = 1$; $T_{G1} = T_{G2} = T_{G3}$= 0.08; $K_{T1} = K_{T2} = 1$; $T_{T1} = T_{T2} = T_{T3}$= 0.3; K_{Psi}= 120; T_{Psi}= 20; $K_{GH} = T_{GH}$ = 85; K_{RS} = 5; T_{RS} = 0.513; T_W = 1; K_B = 1; K_t = 1; K_g = 0.5; T_t = 1.25; Tg = 0.5; G = 1; A = 0.08; B = 0.8 ; F = 0.1; K_{SG} = 1 ; T_{SG} = 0.08 ; R = 4.9801; K_G = 120; T_G = 20, T_{ij}= 0.0707 puMW/rad.

References

[1] Arya, Y., Kumar, N., Dahiya, P., et al., "Cascade- $I\lambda D\mu N$ controller design for AGC of thermal and hydro- thermal power systems integrated with renewable energy sources", *IET Renewable Power Generation*, **15**(3) pp. 504-520 (2021).

[2] Chakrabarti, A. and Halder, S., "Power system analysis: operation and control", In *PHI Learning Pvt. Ltd*, 4th Edn, INDIA, (2022).

[3] Bhagat, S.K., Saikia, L.C. and Babu, N.R., "Effect of partial loading on a three- area hydro- thermal system integrated with realistic dish- Stirling solar thermal system, accurate model of high- voltage direct link considering virtual inertia and energy storage systems.", *International Transactions on Electrical Energy Systems*, **31**(12) p.e13169 (2021).

[4] Kler, D., Kumar, V. and Rana, K.P., "Optimal integral minus proportional derivative controller design by evolutionary algorithm for thermal-renewable energy hybrid power systems", *IET Renewable Power Generation.* **13**(11) pp. 2000–2012 (2019).

[5] Mudi, J., Shiva, C.K., Vedik, B., et al., “Frequency stabilization of solar thermal-photovoltaic hybrid renewable power generation using energy storage devices”, *Iranian Journal of Science and Technology*, **45**(2) pp. 597–617 (2021).

[6] Marimuthu, P., Rajesh, T., Rajeswaran, N., et al., “Comparative Performance Analysis of Deregulated Hydrothermal System with Dual Mode Controller and Diverse Source of Generation Employing Imperialistic Competition Algorithm”, IEEE *Access*, **10** pp. 51008-51020 (2022).

[7] Tasnin, W. and Saikia, L.C., “Deregulated AGC of multi-area system incorporating dish-stirling solar thermal and geothermal power plants using fractional order cascade controller”, *International Journal of Electrical Power & Energy Systems*, **101** pp. 60–74 (2018).

[8] Kumar, R. and Sharma, V.K., “Whale optimization controller for load frequency control of a two-area multi-source deregulated power system”, *International Journal of Fuzzy Systems*, **22**(1) pp. 122-137 (2020).

[9] Biswas, S., Roy, P.K. and Chatterjee, K., "Development of MADB of P- I controller using LMI technique in a renewable energy based AGC system and study its application in a deregulated environment including energy storage device." *Optimal Control Applications and Methods,* **44**(2) pp. 426-451 (2023).

[10] Lei, X., Shang, Y., Shao, Z., et al. “Grid integration of electric vehicles for optimal marginal revenue of distribution system operator in spot market”, *Energy Reports* **8** pp.1061-1068 (2022).

[11] Arya, Y., “A new optimized fuzzy FOPI-FOPD controller for automatic generation control of electric power systems”, *Journal of the Franklin Institute,* **356**(11) pp. 5611–5629 (2019).

[12] Çelik, E., "Performance analysis of SSA optimized fuzzy 1PD-PI controller on AGC of renewable energy assisted thermal and hydro-thermal power systems.", *Journal of Ambient Intelligence and Humanized Computing,* **13**(8) pp. 4103-4122 (2022).

[13] Barisal, A.K., Panigrahi, T.K. and Mishra, S., “A hybrid PSO-LEVY flight algorithm based fuzzy PID controller for automatic generation control of multi area power systems: Fuzzy based hybrid

PSO for automatic generation control", *International Journal of Energy Optimization and Engineering*, **6**(2) pp. 42–63 (2017).

[14] Gheisarnejad, M., "An effective hybrid harmony search and cuckoo optimization algorithm based fuzzy PID controller for load frequency control", Applied *Soft Computing*. **65** pp. 121– 138 (2018).

[15] Rajesh, K.S., Dash, S.S. and Rajagopal, R., "Hybrid improved firefly-pattern search optimized fuzzy aided PID controller for automatic generation control of power systems with multi-type generations", *Swarm and evolutionary computation*, **44** pp. 200–211 (2019).

[16] Sahu, P.C., Prusty, R.C. and Sahoo, B.K., "Modified sine cosine algorithm-based fuzzy-aided PID controller for automatic generation control of multiarea power systems", *Soft Computing* **24**(17) pp. 12919-12936 (2020).

[17] Yumuk, E., Güzelkaya, M. and Eksin, I., "Reduced inverse integer-order controller design for a class of fractional-order model: Case study on two-tank liquid-level process", *Proceedings of the Institution of Mechanical Engineers, Part I: Journal of Systems and Control Engineering,* **237**(5) pp. 815-823 (2023).

[18] Guha, D., Roy, P.K. and Banerjee, S., "Adaptive fractional-order sliding-mode disturbance observer-based robust theoretical frequency controller applied to hybrid wind–diesel power system", *ISA transactions*, **133** pp. 160-183 (2023).

[19] Arya, Y. and Kumar, N., "BFOA-scaled fractional order fuzzy PID controller applied to AGC of multi-area multisource electric power generating systems", *Swarm and Evolutionary Computation,* **32** pp. 202–218 (2017).

[20] Kumar, A., Kumari, N., Shankar, G., et al. "Load Frequency Control of Distributed Generators Assisted Hybrid Power System Using QOHSA Tuned Model Predictive Control", *IEEE Access*, **10** pp. 109311-109325 (2022).

[21] Arya, Y., "A novel CFFOPI-FOPID controller for AGC performance enhancement of single and multi-area electric power systems", *ISA transactions*, **100** pp. 126–135 (2020).

[22] Saha, A. and Saikia, L.C., “Utilisation of ultracapacitor in load frequency control under restructured STPP-thermal power systems using WOA optimised PIDN-FOPD controller”, *IET Generation, Transmission & Distribution.* **11**(13) pp. 3318–3331 (2017)

[23] Arya, Y., “AGC of PV-thermal and hydro-thermal power systems using CES and a new multi-stage FPIDF-(1+ PI) controller”, *Renewable Energy Elsevier*, **134**(C) pp. 796-806 (2019).

[24] Elsisi, M., “New variable structure control based on different meta-heuristics algorithms for frequency regulation considering nonlinearities effects”, *International Transactions on Electrical Energy Systems.* **30**(7) e12428 (2020).

[25] Elsisi, M., Soliman, M., Aboelela, M.A.S., et al., “GSA based design of dual proportional integral load frequency controllers for nonlinear hydrothermal power system”. *World Academy of Science, Engineering and Technology,* **9** pp. 1142– 1148 (2015).

[26] Goswami, L., Biswas, S., Dutta, S. and Roy, P.K., et al., “Load frequency control of multi area power system with de-regulation using OKHA”, *Third Int. Conf. on Science Technology Engineering & Management (ICONSTEM)*, pp. 507–512 (2017).

[27] Rajesh, K.S. and Dash, S.S., “Load frequency control of autonomous power system using adaptive fuzzy based PID controller optimized on improved sine cosine algorithm”, *Journal of Ambient Intelligence and Humanized Computing.* **10**(6) pp. 2361–2373 (2019).

[28] Abadi, A.S.S., Hosseinabadi, P.A. and Mekhilef, S., “Fuzzy adaptive fixed-time sliding mode control with state observer for a class of high-order mismatched uncertain systems”, *International Journal of Control, Automation and Systems.***18** pp. 2492-508 (2020).

[29] Han, J., Shan, X., Liu, H., Xiao, J., et al., “Fuzzy gain scheduling PID control of a hybrid robot based on dynamic characteristics”, *Mechanism and Machine Theory*, **184** (2023).

[30] Ghamari, S. M., Narm, H. G., and Mollaee, H., “Fractional- order fuzzy PID controller design on buck converter with antlion optimization algorithm”, *IET Control Theory & Applications,* **16**(3) pp. 340-352 (2022).

[31] Schmuck, R., “Adaptive value of aggregation behavior in the fire bug Pyrrhocorisapterus (Heteroptera: Pyrrhocoridae)”. *Entomologia generalis,* **19**(3) pp. 143-156 (1995).

[32] Zdarek, J., “Mating Behaviour in the Bug, Pyrrhocoris Ap Ter Us L.(Heteroptera): Ontogeny and Its Environmental Control”, *Behaviour*, **37**(3-4) pp. 253-268 (1970).

[33] Schöfl, G. and Taborsky, M., “Prolonged tandem formation in firebugs (Pyrrhocorisapterus) serves mate-guarding”. *Behavioral Ecology and Sociobiology*, **52**(5) pp. 426-433 (2002).

[34] Suresh, K., Sreeja Mole, S.S. and Joseph Selva Kumar, A., "F2SO: an energy efficient cluster based routing protocol using fuzzy firebug swarm optimization algorithm in WSN." *The Computer Journal* **66**(5) pp. 1126-1138 (2023).

[35] Noel, M.M., Muthiah-Nakarajan, V., Amali, G.B., et al. “A new biologically inspired global optimization algorithm based on firebug reproductive swarming behavior”, *Expert Systems with Applications,* **183** pp. 115408 (2021).

[36] Gupta, N. and Garg, R., “Tuning 34of asymmetrical fuzzy logic control algorithm for SPV system connected to grid”, *International journal of hydrogen energy,* **42**(26) pp. 16375– 16385 (2017).

[37] Arya, Y., “Automatic generation control of two-area electrical power systems via optimal fuzzy classical controller”, *Journal of the Franklin Institute.* **355**(5) pp. 2662–2688 (2018).

[38] Biswas, S., Roy, P.K. and Chatterjee, K., “Facts-based 3DOF-PID controller for LFC of renewable power system under deregulation using GOA”, *IETE Journal of Research,* **69**(3) pp. 1–14 (2021).

[39] Reams, R., “Hadamard inverses, square roots and products of almost semidefinite matrices”, *Linear Algebra and its Applications,* **288** pp. 35-43 (1999).

[40] Ryser, H.J., “Combinatorial mathematics” *American Mathematical Soc.* **(14)** (1963).

[41] Styan, G.P., “Hadamard products and multivariate statistical analysis”, *Linear algebra and its applications*. **6** pp. 217-240 (1973).

[42] Tripathy, D., Choudhury, N. B. D., and Sahu, B., K., “Grasshopper optimization algorithm-based fuzzy-2DOF-PID controller for LFC of interconnected system with nonlinearities”, *International Journal of Social Ecology and Sustainable Development,* **12**(3) pp. 11-29 (2021).

[43] Mishra, S., Nayak, P.C., Prusty, R.C. and Panda, S., “Performance analysis of multistage PID controller for frequency regulation of multi microgrid system using atom search optimization”, International *Journal of Ambient Energy*, **43**(1) pp. 7371-7386 (2022).

[44] Arya, Y., "ICA assisted $FTI\lambda DN$ controller for AGC performance enrichment of interconnected reheat thermal power systems." *Journal of Ambient Intelligence and Humanized Computing*, **14**(3) pp. 1919-1935 (2023).

Figure captions:

Figure 1 Block diagram of two-area hybrid test system (thermal-hydro-gas) [11]

Figure 2 Fuzzy inference system

Figure 3 Distribution of MFs for ACE, ACE-D & FLC

Figure 4 Surface generation of Fuzzy inference system [36]

Figure 5 Comparative assessment of Q with ISE

Figure 6 Block Diagram of 3DOF-PID Controller [38]

Figure 7 Block Diagram of Fuzzy-3DOF-PID Controller

Figure 8 Modeling of the movement of Firebugs

Figure 9 FSO Flowchart

Figure 10 (a) Frequency deviation in area 1 **(b)** Frequency deviation in area 2 **(c)** Tie-bar power error of the system

Figure 11 Linearized model of 3-area ocean thermal hybrid power system

Figure 12 (a) Deviation of Frequency in area 1 **(b)** Deviation of Frequency in area 2 **(c)** Deviation of Frequency in area 3 **(d)** Ocean-Thermal Unit Error **(e)** Tie-bar power error between 1st and 2nd area **(f)**

Tie-bar power error between 1st and 3rd area (All results are obtained using four different controllers tuned by FSO algorithm under influence of 10% SLP load)

Figure 13 (a) Deviation of Frequency in area 1 **(b)** Deviation of Frequency in area 2 **(c)** Deviation of Frequency in area 3 **(d)** Tie-bar power error between 1st and 2nd area **(e)** Tie-bar power error between 1st and 3rd area (All results are obtained using Fuzzy-3DOF-PID controller under influence of 10% SLP load)

Figure 14 Frequency deviation in Ocean-Thermal unit under ±0.02 puMw RLP type load

Figure 15 Frequency deviation in area-2 with $\pm 20\%$ variation in system parameters

Table captions:

Table 1 Taxonomy of the publications regarding LFC using different controller and algorithm

Table 2. Rule base for ACE, ACE Derivatives and FLC output [36]

Table 3 FSO tuned PID, FOPID, 3DOF-PID controller parameters for 2 area system

Table 4 Undershoot (US), overshoot (OS) and settling time (ST) using FSO tuned PID, FOPID, FUZZY-PID & FUZZY-3DOF-PID Controller

Table 5 Undershoot (US), overshoot (OS) and settling time (ST) using FSO tuned PID, FOPID, FUZZY-PID & FUZZY-3DOF-PID Controller

Table 6 FSO tuned PID, FOPID, 3DOF-PID controller parameters for hybrid 3 area power system

Table 7 GOA, ICA, ASO, FSO tuned 3DOF-PID controller parameters for 3-area system

Table 8 Undershoot (US), overshoot (OS) and settling time (ST) using GOA, ICA, ASO, FSO tuned FUZZY-3DOF-PID Controller

Table 9 Numerical values of Q_s (20 seconds) for different controlling units

Table 10 Parameter variation for system stability

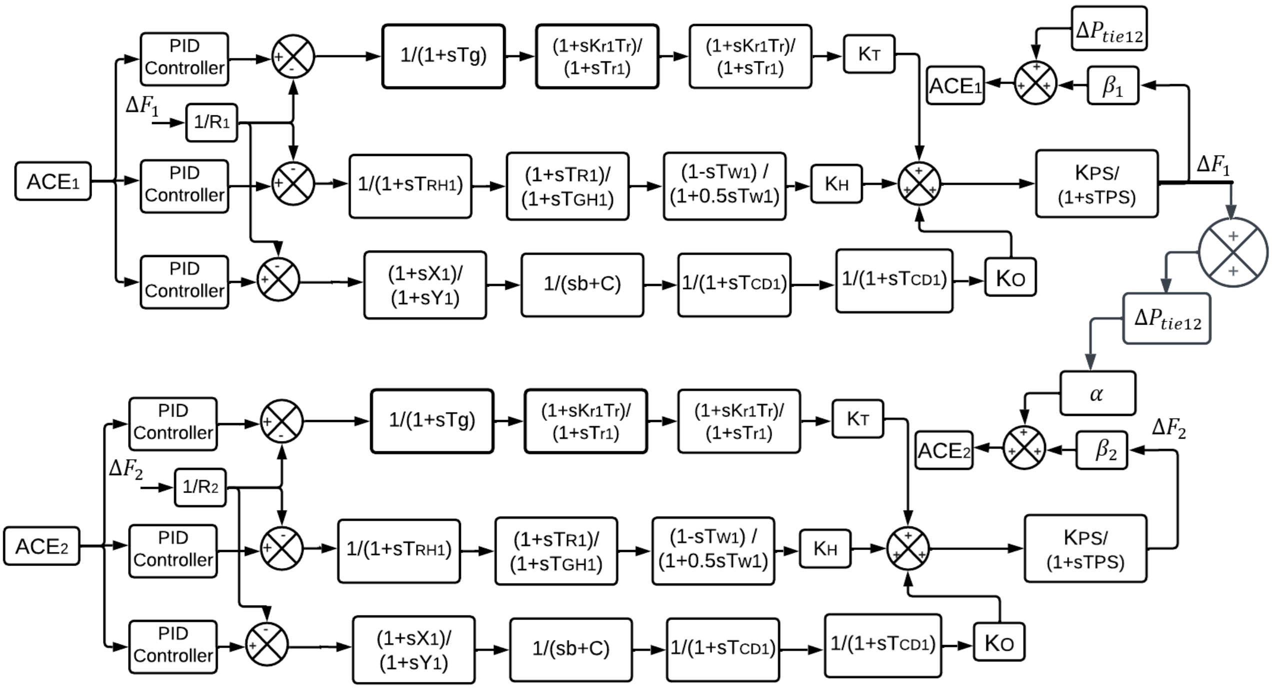

Figure 1

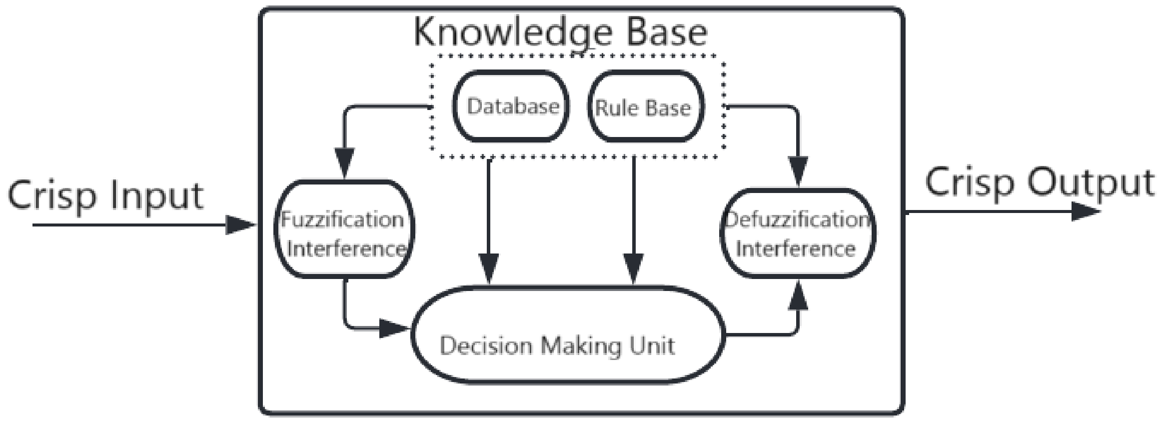

Figure 2

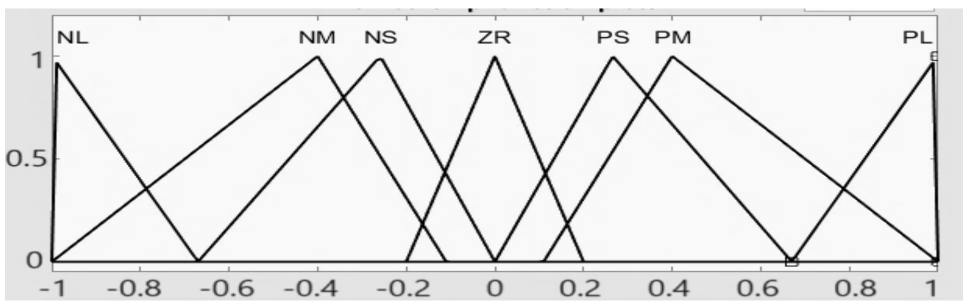

Figure 3

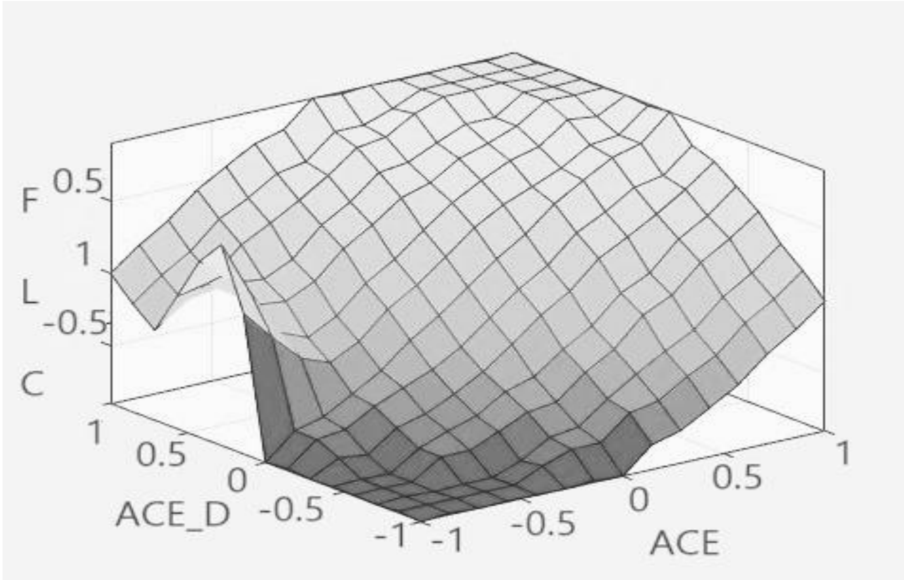

Figure 4

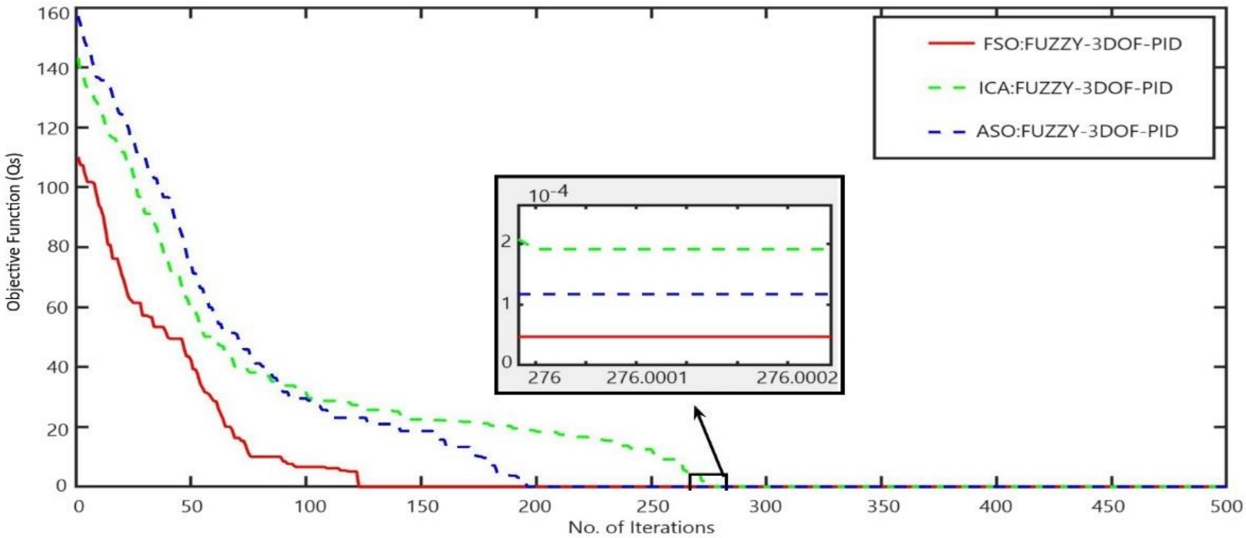

Figure 5

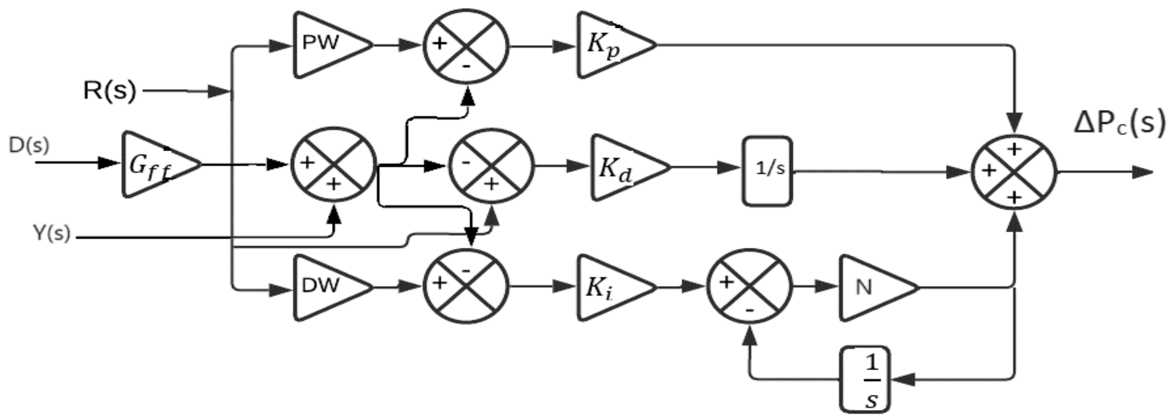

Figure 6

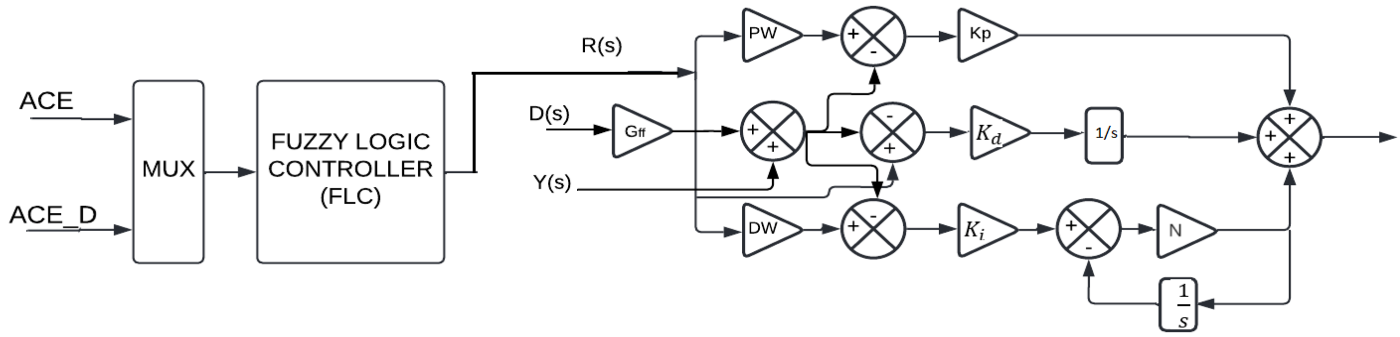

Figure 7

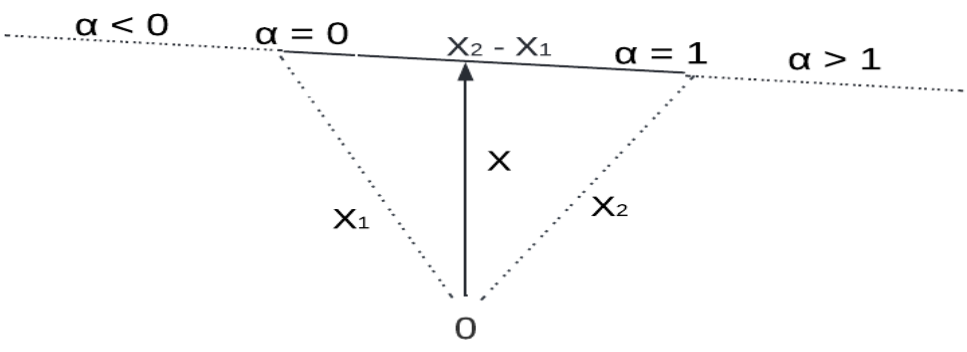

Figure 8

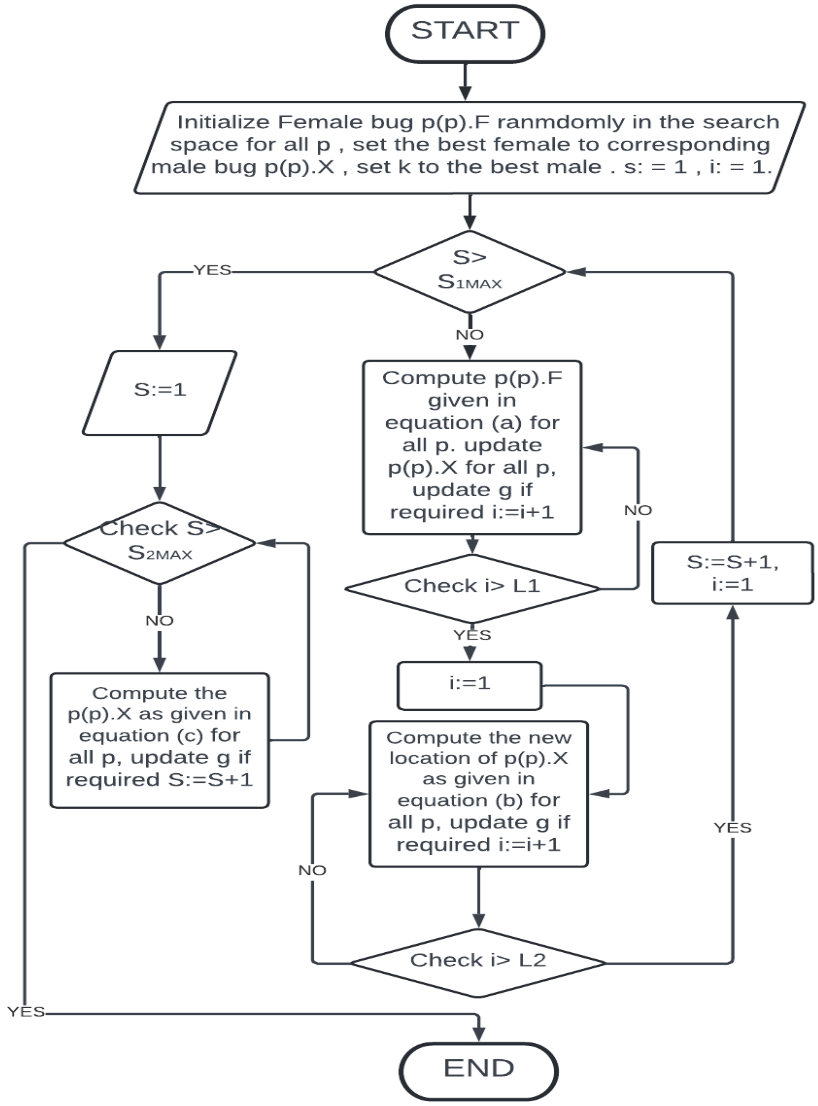
START
Initialize Female bug p(p).F ranmdomly in the search space for all p , set the best female to corresponding male bug p(p).X , set k to the best male . s: = 1 , i: = 1.
S> S1MAX
YES
NO
S:=1
Compute p(p).F given in equation (a) for all p. update p(p).X for all p, update g if required i:=i+1
NO
Check S> S2MAX
Check i> L1
S:=S+1, i:=1
NO
YES
i:=1
Compute the p(p).X as given in equation (c) for all p, update g if required S:=S+1
Compute the new location of p(p).X as given in equation (b) for all p, update g if required i:=i+1
YES
NO
Check i> L2
YES
END

Figure 9

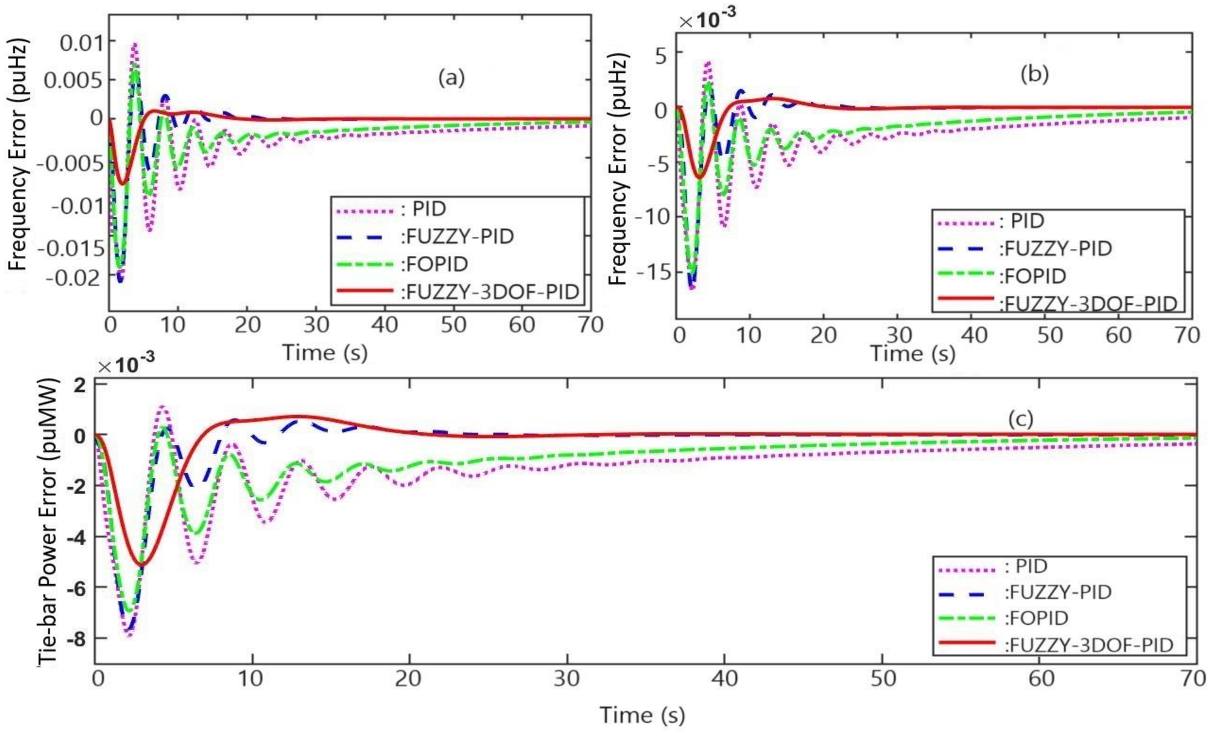
(a)
Frequency Error (puHz)
Time (s)
: PID
:FUZZY-PID
:FOPID
:FUZZY-3DOF-PID
(b)
×10^-3
Frequency Error (puHz)
Time (s)
: PID
:FUZZY-PID
:FOPID
:FUZZY-3DOF-PID
(c)
×10^-3
Tie-bar Power Error (puMW)
Time (s)
: PID
:FUZZY-PID
:FOPID
:FUZZY-3DOF-PID

Figure 10

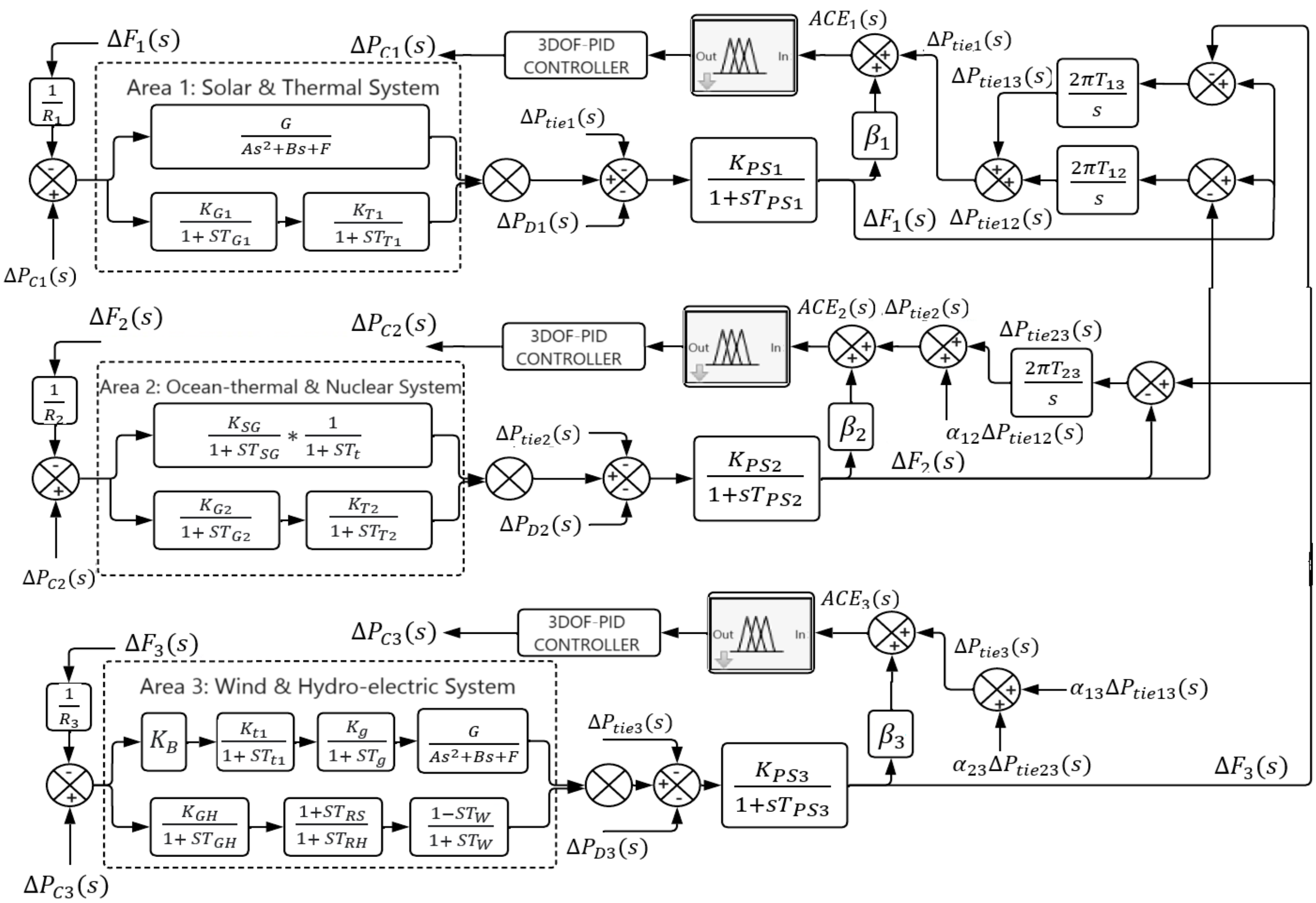
Area 1: Solar & Thermal System
Area 2: Ocean-thermal & Nuclear System
Area 3: Wind & Hydro-electric System
3DOF-PID CONTROLLER
3DOF-PID CONTROLLER
3DOF-PID CONTROLLER
Out
In
ΔF1(s)
ΔPC1(s)
ΔPtie1(s)
ΔPD1(s)
ACE1(s)
ΔPtie13(s)
ΔPtie12(s)
ΔF2(s)
ΔPC2(s)
ΔPtie2(s)
ΔPD2(s)
ACE2(s)
ΔPtie23(s)
α12ΔPtie12(s)
ΔF3(s)
ΔPC3(s)
ΔPtie3(s)
ΔPD3(s)
ACE3(s)
α13ΔPtie13(s)
α23ΔPtie23(s)

Figure 11

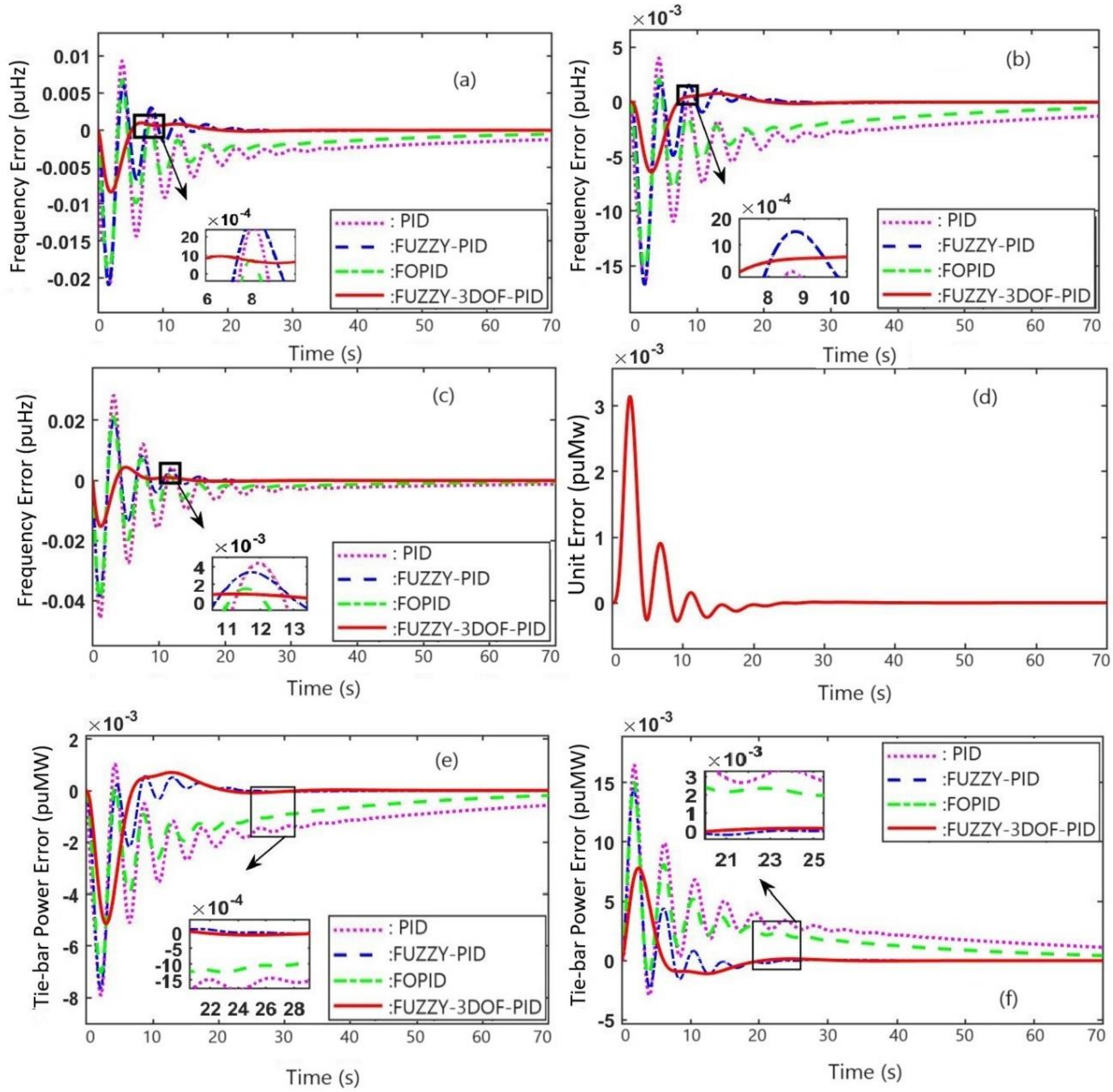

Figure 12

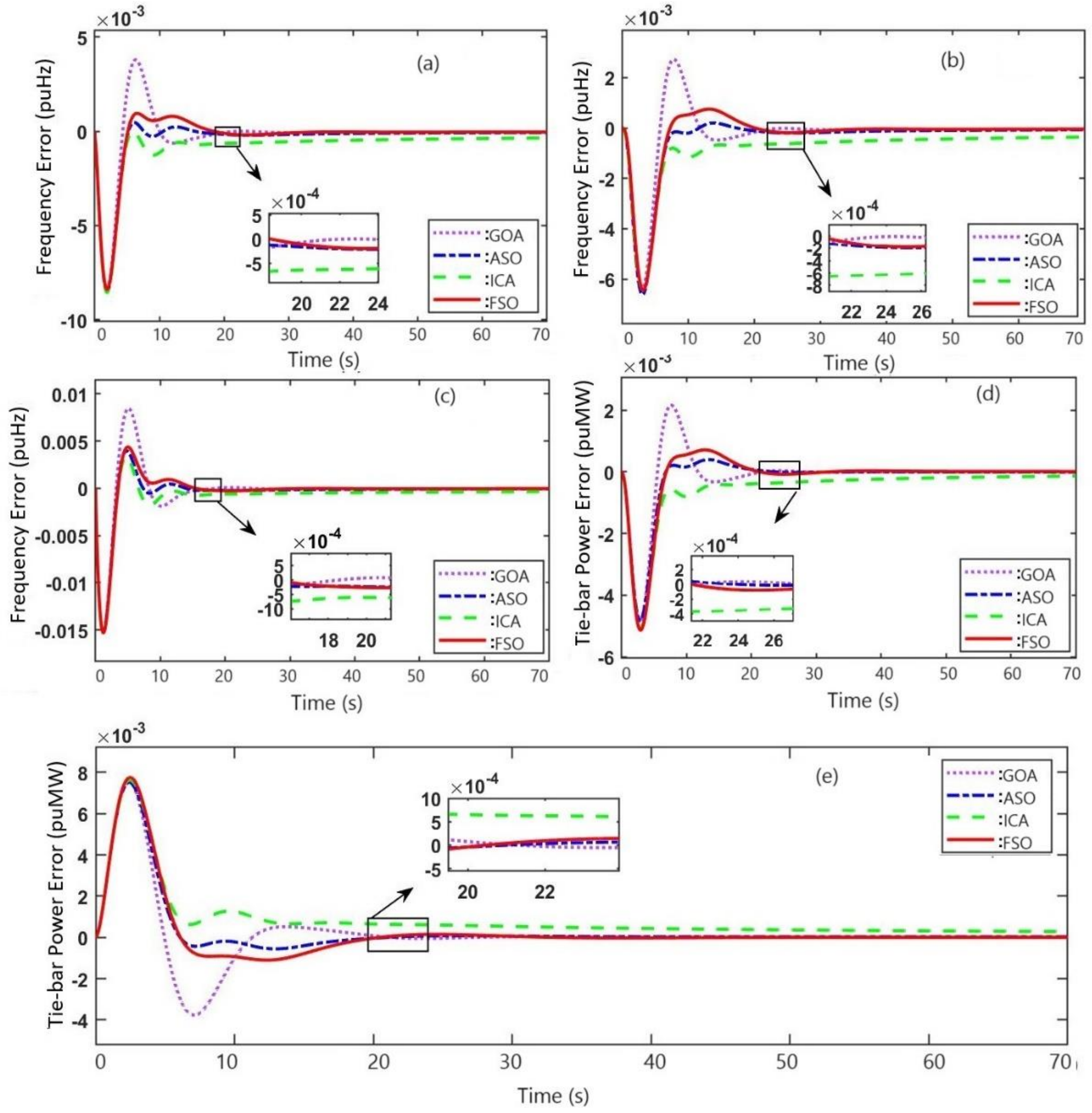

Figure 13

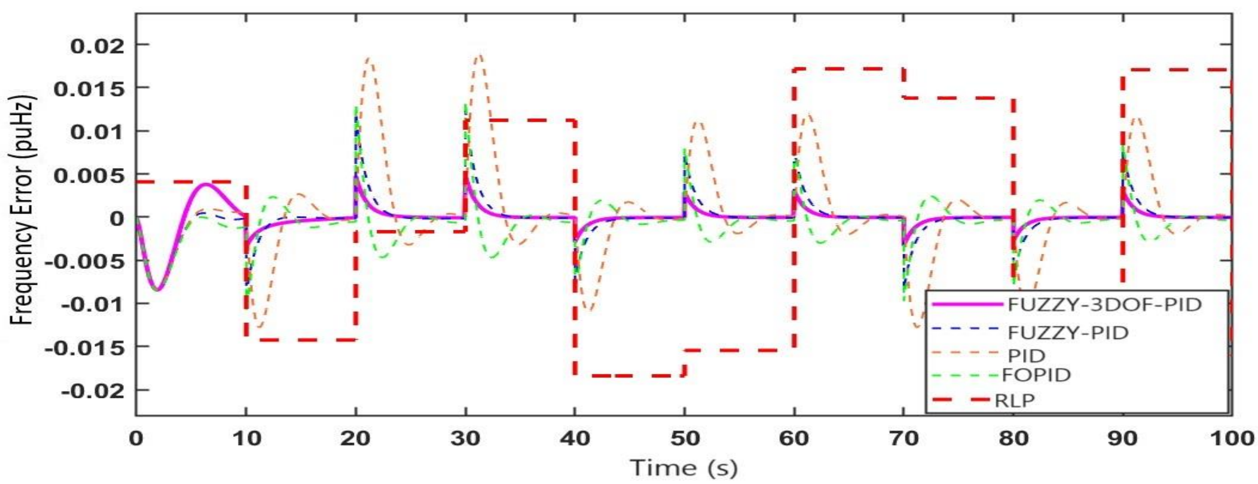

Figure 14

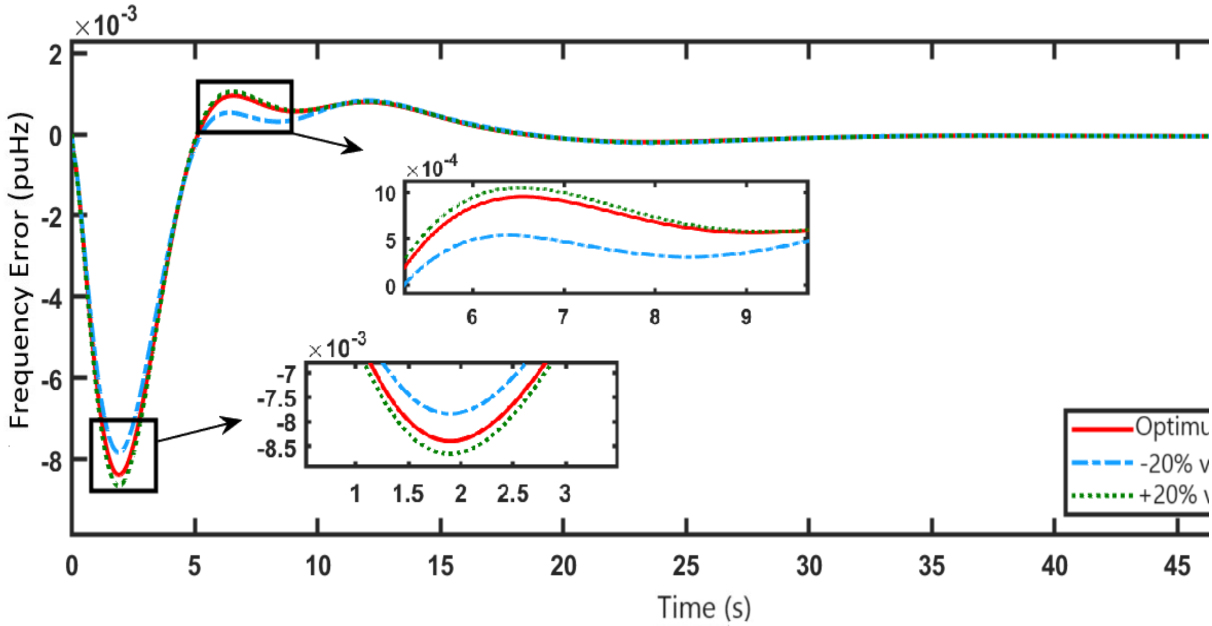

Figure 15

Table 1

References	Thermal	Nuclear	Hydroelectric	Gas	Solar	Wind	Ocean thermal	Area Type	PI	PID	3DOF-PID	FOPID	FUZZY based PI	FUZZY based PID	FUZZY based FOPID	Algorithm
	AGC SYSTEMS								**CONTROLLERS**							
9	✓		✓	✓	✓	✓		2	✓							CASO
11	✓		✓					3							✓	ICA
23	✓		✓		✓			2						✓		ICA
24	✓		✓	✓				2		✓						BFA
25	✓		✓					2	✓							GSA
27					✓	✓		2						✓		SCA
37	✓		✓		✓			2					✓			ICA
38	✓		✓	✓	✓	✓		2			✓					GOA
44	✓							2						✓		ICA
Present Work	✓	✓	✓		✓	✓	✓	**3**						✓	✓	**FSO**

Table 2

	ACE DERIVATIVES(ACE-D)						
ACE	**NL**	**NM**	**NS**	**ZR**	**PS**	**PM**	**PL**
NL	NL	NL	NL	NL	NM	NS	ZR
NM	NL	NL	NL	NM	NS	ZR	PS
NS	NL	NL	NM	NS	ZR	PS	PM
ZR	NL	NM	NS	ZR	PS	PM	PL
PS	NM	NS	ZR	PS	PM	PL	PL
PM	NS	ZR	PS	PM	PL	PL	PL
PL	ZR	PS	PM	PL	PL	PL	PL

Table 3

Tuned	PID	FOPID	3DOF-PID
K_{p1}	0.01255	5.4897	1.532
K_{p2}	0.0245	0.0274	0.0274
K_{d1}	0.4856	5.851	1.0625
K_{d2}	0.9433	0.01	0.0128
K_{i1}	3.7786	3.7741	1.3411
K_{i2}	0.033	0.021	0.013
μ_1	-	0.72	-
μ_2	-	0.72	-
λ_1	-	0.965	-
λ_2	-	0.965	-
PW	-	-	112.46
DW	-	-	1.1025
N	-	-	0.2591

Table 4

		Two-area test system			
Functions	**Parameters**	**PID**	**FOPID**	**FUZZY-PID**	**FUZZY-3DOF-PID**
	OS	0.00954	0.00594	0.00702	0.000961
ΔF_1	US	-0.0209	-0.02095	-0.01909	-0.00840
	ST	-	-	22.31	20.56
	OS	0.00415	0.001754	0.002301	0.000753

ΔF_2	US	-0.0167	-0.01669	-0.01554	-0.00643
	ST	-	-	22.16	20.11
	OS	0.00112	0.000585	0.000303	0.000714
ΔP_{tie12}	US	-0.0792	-0.00765	-0.00696	-0.00513
	ST	-	-	21.45	20.06

Table 5

Three area hybrid system					
Functions	**Parameters**	**PID**	**FOPID**	**FUZZY-PID**	**FUZZY-3DOF-PID**
	OS	0.00934	0.00596	0.00679	0.000952
ΔF_1	US	-0.0209	-0.0209	-0.0192	-0.00839
	ST	-	-	22.31	20.56
	OS	0.0040	0.0018	0.0021	0.00076
ΔF_2	US	-0.017	-0.0167	-0.0153	-0.00644
	ST	-	-	22.14	20.12
	OS	0.0283	0.0205	0.0002	0.00437
ΔF_3	US	-0.046	-0.039	-0.04	-0.0154
	ST	-	-	22.16	14.51
	OS	0.0011	0.0006	0.0002	0.0007
ΔP_{tie12}	US	-0.008	-0.008	-0.007	-0.005
	ST	-	-	22.52	20.83
	OS	0.0165	0.0145	0.015	0.008
ΔP_{tie13}	US	-0.0029	-0.0023	-0.0013	-0.0011
	ST	-	-	22.48	20.46

Table 6

Tuned Parameter	**PID**	**FOPID**	**3DOF-PID**
K_{p1}	0.01	5.845	1.532
K_{p2}	0.01	0.01	0.0274
K_{p3}	0.01	0.01	0.0146
K_{d1}	0.46773	5.856	1.0625
K_{d2}	0.92378	0.01	0.0128
K_{d3}	0.01	0.01	0.01
K_{i1}	3.6593	3.6586	1.3411
K_{i2}	0.01	0.01	0.013
K_{i3}	0.01	0.10243	0.5211
μ_1	-	0.7	-
μ_2	-	0.7	-

μ_3		0.7	
λ_1	-	0.965	-
λ_2	-	0.965	-
λ_3		0.965	
PW	-	-	112.46
DW	-	-	1.1025
N	-	-	0.2591

Table 7

Optimized parameters	GOA	ICA	ASO	FSO
K_{p1}	5.644	6.025	6.025	1.532
K_{p2}	0.015	0.022	0.02	0.0274
K_{p3}	0.011	0.02	0.02	0.0146
K_{d1}	5.864	5.993	6.020	1.0625
K_{d2}	0.015	0.03	0.01	0.0128
K_{d3}	0.013	0.03	0.01	0.01
K_{i1}	3.606	3.602	3.68	1.3411
K_{i2}	0.012	0.03	0.01	0.013
K_{i3}	0.102	0.144	0.156	0.5211
PW	110.66	115.7	114.58	112.46
DW	1.1487	1.1443	1.0952	1.1025
N	0.2486	0.2587	0.2611	0.2591

Table 8

Three area hybrid system					
Functions	**Parameters**	**GOA**	**ICA**	**ASO**	**FSO**
	OS	0.00377	0.000796	0.000225	0.000952
ΔF_1	US	-0.00842	-	-0.00859	-0.008390
	ST	-	-	22.61	20.56
	OS	0.00271	0.000667	0.00	0.000752
ΔF_2	US	-	-0.00646	-0.00642	-0.006403
	ST	-	-	20.14	20.12
	OS	0.00845	0.004225	0.003358	0.004371
ΔF_3	US	-0.0153	-0.01524	-0.01537	-0.01532
	ST	29.85	54.46	17.28	14.51
	OS	0.00216	0.00056	0.00	0.0007111

ΔP_{tie12}	US	-	-	-0.00507	-0.005139
	ST	34.22	-	28.04	20.83
	OS	0.00755	0.007574	0.007611	0.007761
ΔP_{tie13}	US	-	-0.00103	0.00	-0.001104
	ST	28.50	-	21.86	20.46

Table 9

Controller type	**Objective functions (Q_s)**			
	ISE	**ITSE**	**IAE**	**ITAE**
FSO: PID	0.0766	0.0812	0.1823	0.2751
FSO: FOPID	0.00992	0.00806	0.0472	0.0227
GOA:FUZZY-3DOF-PID	0.000226	0.00113	0.0072	0.0862
ICA:FUZZY-3DOF-PID	0.000191	0.000111	0.0069	0.0472
ASO:FUZZY-3DOF-PID	0.000117	0.000098	0.0093	0.0371
FSO:FUZZY-PID	0.00106	0.000447	0.0921	0.0930
FSO:FUZZY-3DOF-PID	**0.0000468**	**0.0000227**	**0.0062**	**0.0104**

Table 10

System Parameters	Optimum Value	Parameter Variation	
		$+20\%$	-20%
K_{SG}	1	1.2	0.8
T_{SG}	0.08	0.096	0.064
T_t	1.25	1.5	1
K_{G2}	1	1.2	0.8
T_{G2}	0.08	0.096	0.064
K_{T2}	1	1.2	0.8
T_{T2}	0.3	0.36	0.24

Susmit Chakraborty was born in Kolkata, West Bengal, India in 1994. obtained M.Tech degree in Power Electronics and Electrical Drives from Indian Institute of Technology (ISM) Dhanbad in 2020. Presently, he is working as an Assistant Professor in Electrical & Electronics Engineering Department at Pailan College of Management & Technology, West Bengal, India. His research interest includes Load Frequency Control, Power system stability, operation and its control etc.

Arindam Mondal was born in Baruipur, West Bengal, India in 1980. He obtained PhD degree in Electrical Engineering from National Institute of Technical Teachers Training & Research ,Kolkata in 2017. Presently, he is working as a Professor in Electrical Engineering Department at Dr. B.C Roy Engg College, West Bengal, India. His research interest includes system idenfication , fractional order control and signal processing , IoT, Bio-informatics ,Load Frequency Control etc.

Soumen Biswas was born in Kalyani,West Bengal, India in 1986. He obtained PhD degree in Electrical Engineering from Indian Institute of Technology (ISM) Dhanbad in 2022. He is working Assistant professor in Electrical Engineering Department at Dr. B.C Roy Engg College, West Bengal, India. His research interest includes FACTS, automatic generation control, deregulated power system stability, evolutionary computing techniques, etc.

Provas Kumar Roy obtained PhD degree in Electrical Engineering from National Institute of Technology Durgapur in 2011. Presently, he is working as a Professor in Electrical Engineering Department at Kalyani Government Engineering College, West Bengal, India. His research interest includes economic load dispatch, optimal power flow, FACTS, automatic generation control, radial distribution network, power system stabilizer, image processing, machine learning, evolutionary techniques, etc.